From Department of Physiology and Pharmacology
Karolinska Institutet, Stockholm, Sweden

SINGLE-CELL TRANSCRIPTOMIC ANALYSES OF EARLY EMBRYONIC DEVELOPMENT AND DEVELOPMENTAL PROGRAMMING BY ANDROGEN EXCESS

Yu Pei

Karolinska Institutet

Stockholm 2022

Published by Karolinska Institutet.
Printed by Universitetsservice US-AB, 2022

ISBN 978-91-8016-749-9

Single-cell transcriptomic analyses of early embryonic development and developmental programming by androgen excess
THESIS FOR DOCTORAL DEGREE (Ph.D.)

By

Yu Pei

The thesis will be defended in public at Ragnar Granit, Biomedicum, Karolinska Institutet, Stockholm, 9th of September at 13:00.

Principal Supervisor:
Associate Professor: Qiaolin Deng
Karolinska Institutet
Department of Physiology and Pharmacology

Co-supervisor(s):
Professor: Elisabet Stener-Victorin
Karolinska Institutet
Department of Physiology and Pharmacology

Professor Johan Ericson
Karolinska Institutet
Department of Cell and Molecular Biology

Senior Researcher: Daniel Ramsköld
Karolinska Institutet
Department of Cell and Molecular Biology

Opponent:
Professor: Matti Poutanen
University of Turku
Department of Physiology

Examination Board:
Associate Professor: Pauliina Damdimopoulou
Karolinska Institutet
Department of Clinical Science, Intervention and Technology

Professor: Kenny Rodriguez-Wallberg
Karolinska Institutet
Department of Oncology-Pathology

Associate Professor: Masoud Zamani Estek
University of Maastricht
Department of Clinical Genetics

To my beloved family

ABSTRACT

Infertility is a compelling problem an increased prevalence among couples. Although multiple causes have been hypothesized to increase the risk of infertility, changes in lifestyles and environment are the possible links to the causes. While germ cells represent the eternal link between generations, epigenetic modification in germ cells provides a conceivable link between the environmental influences and alterations in gene expression across generations. During embryonic development, there are several important processes that can affect fertility, including germ cell specification, germ cell migration along hindgut, germ cell localization at gonads, sex differentiation and further stages of gametogenesis. We are particularly interested in polycystic ovarian syndrome (PCOS) as it is the main cause of infertility worldwide. PCOS is highly heritable, with estimated 70% familial heritability. However, in total, 19 loci significantly linked to PCOS from genome-wide association studies (GWAS) only account for ~10% of its heritability. Recent studies suggest that epigenetic regulation of embryonic development and germline modification resulting from hyperandrogenism in the uterine environment contribute to the onset of PCOS in offspring and across generations.

This thesis includes three studies to understand the possible causes related to infertility during early embryonic development and germline. The aim of **Study I** is to investigate cellular heterogeneity of epiblast during early embryonic development by single-cell transcriptomic analysis. The aim of **Study II** is to investigate whether prenatal androgen exposure leads to transgenerational transmission of PCOS. The aim of **Study III** is to study molecular effects of fetal and adult programming by androgen in different PCOS-like mouse models as well as a maternal obesity mouse model by transcriptional profiling of key organs.

LIST OF SCIENTIFIC PAPERS

I. Single-Cell RNA-Seq Reveals Cellular Heterogeneity of Pluripotency Transition and X Chromosome Dynamic during Early Mouse Development. Cheng S*, **Pei Y***, He L, Peng G, Reinius B, Tam PPL, Jing N, Deng Q. Cell Rep. 2019 Mar 5; 26(10):2593-2607

II. Prenatal androgen exposure and transgenerational susceptibility to polycystic ovary syndrome. Risal S*, **Pei Y***, Lu H*, Manti M, Fomes R, Pui HP, Zhao Z, Massart J, Ohlsson C, Lindgren E, Crisosto N, Maliqqueo M, Echiburu B, Ladron de Guevara A, Sir-Petemann T, Larsson H, Rosenqvist MA, Cesta CE, Benrick A, Deng Q, Stener-Victorin E. Nature Medicine 25, 1894-1904(2019)

III. Transcriptomic mapping of key reproductive and metabolic tissues and oocytes in mouse models of polycystic ovary syndrome. **Pei Y***, Risal S*, Jiang H, Lu H, Lindgren E, Stener-Victorin E*, Deng D*. (Manuscript)

* Equal Contribution

PUBLICATIONS NOT INCLUDE IN THIS THESIS

I. Single-Cell Analysis Reveals Major Histocompatibility Complex II–Expressing Keratinocytes in Pressure Ulcers with Worse Healing Outcomes. Li D, Cheng S, **Pei Y**, Sommar P, Kärner J, Heter E, Toma M, Zhang L, Pham K, Cheung Y, Liu Z, Chen X, Deng Q, Landen X. J Invest Dermatol. 2021 Sep 16. Doi: 10.1016/j.jid.2021.07.176

II. GABA Regulates Release of Inflammatory Cytokines From Peripheral Blood Mononuclear Cells and CD4 + T Cells and Is Immunosuppressive in Type 1 Diabetes. Bhandage AK, Jin Z, Korol SV, Shen Q, **Pei Y**, Deng Q, Espes D, Carlsson PO, Kamali-Moghaddam M2, Birnir B. EBioMedicine. 2018 Apr; 30:283-294.

CONTENTS

LIST OF ABBREVIATIONS

AKT1	AKT serine/Threonine kinase 1
AMN	Amnion associated transmembrane protein
AP2γ (TFAP2C)	Transcription factor-2 gamma
AR	Androgen receptor
ASCL2	Achaete-scute family BHLH transcriptioin factor 2
AVE	Anterior visceral endoderm
BMP15	Bone morphogenetic protein 15
BMP4	Bone morphogenetic protein 4
CXCR4	Chemokine receptor type 4
CYP11A1	Cytochrome P450, family 11, member A1
DAX1	Dosage sensitive sex reversal, adrenal hypoplasia critical region, on chromosome X, gene1
DHT	Dihydrotestosterone
DND1	Dead-end protein homolog 1
DNMT3A	DNA methyltransferase 3 alpha
DNMT3B	DNA methyltransferase 3 beta
DNMT3L	DNA methyltransferase 3 like
DOHaD	Developmental origins of health and disease
DPPA4	Developmental pluripotency associated 4
EOMES	Eomesodermin
EpiLCs	epiblast-like cells
EpiSCs	epiblast stem cells
ESC	Embryonic stem cells
EXE	Extraembryonic ectoderm
FABP5	Fatty acid binding protein 5
FGF	Fibroblast growth factor
FOLLISTATIN	Female differentiation factors
FSH	Follicle-stimulating
GDF9	Growth and differentiation factor 9
GnRH	Gonadotropin-releasing hormones

HFHS	high fat/high sucrose
INIP	INTS3 and NABP interacting protein
INTS3	Integrator complex subnuit 3
KITL	Stem cell growth factor ligand
LH	Luteinizing hormone
MCM-2	Minichromosome maintenance complex component 2
MIXL1	Mix paired-like homeobox
NANOS3	Nanos C2HC-Type Zinc Finger 3
NGF	Nerve growth factor
NGS	Next-generation sequencing
PCOM	Polycystic ovarian morphology
PCOS	Polycystic ovarian syndrome
PE	Primitive endoderm
PGC	Primodial germ cell
PNA	Prenatal androgen
POGZ	Pogo transposable elment derived with ZNF domain
POU5F1	Pou class 5 homeobox1
PRDM(BLIMP1)	PR domain zinc-finger protein 1
PRDM14	PR domain zinc-finger protein 14
RA	Retinoic acid
RHOA	Ras homolog family member A
RNF141	Ring finger protein 141
SDF1	Stromal cell-derived factor 1
SHBG	Sex hormone binding globin
STRA8	Stimulated by retinoic acid 8
TET	Ten-eleven translocation proteins
TGFB	Transforming growth factor-beta family cytokines
TIAL1	TIA1 cytotoxic granule associated RNA binding protein like 1
TMEM214	Transmembrane protein 214
UHRF1	Ubiquitin like with PHD and ring finger domains 1
WNT3	Wnt family member 3

WNT4	Wnt family member 4
XCI	X chromosome inactivation
XCR	X chromosome reactivation

1 INTRODUCTION

1.1 EARLY MOUSE EMBRYONIC DEVELOPMENT

The mouse embryonic development is a dynamic and self-organized process. From a fertilized egg to a gastrulation embryo, it comprises a tightly regulated set of lineage specification processes as well as simultaneous establishment of the embryonic axes (**Fig.1**) (Rossant and Tam, 2009). These processes involve the formation of a blastocyst at embryonic day (E3.5), followed by compaction during which the cells segregate to form trophectoderm (TE), or inner cell mass (ICM), and along with time, form primitive endoderm (PE) and the epiblast (EPI) from ICM. Blastocysts comprise of the EPI, the extraembryonic primitive endoderm and the trophectoderm three cell types. Blastocyst implantation commences a conversation between the uterus and the embryo, enabling the reorganization of both the maternal tissues and the embryo (Bedzhov et al., 2014). From embryonic day (E4.5) to embryonic day (E6.5), epiblast cells quickly proliferate and reorganize into a cup-shaped columnar epithelium before gastrulation. The pluripotent EPI serves as the foundation for patterning and specification of germ layers and the germline that build the embryo proper. Various important steps are involved in establishing gastrulation including specification of germ layer progenitors; establishment of the embryonic axes and coordinating with tissue movements (Tam et al., 2006). Moreover, the inductive signal interactions between extra-embryonic cells and embryonic cells are important for embryonic patterning and lineage specification.

Prior to gastrulation, the post-implantation mouse embryo exhibits distinctive morphological asymmetries such as the establishment of anterior-posterior (A-P) asymmetry. WNT, NODAL signaling pathways in the visceral endoderm (VE) which forms from PE could contribute to the establishment of A-P axis in pre-gastrula embryos and positioning the primitive streak (Rossant and Tam, 2004). Wnt family member 3 (*Wnt3*) expression in the posterior epiblast demarcates the identity of EPI which later denotes the formation of primitive streak during gastrulation (Rivera-Pérez and Magnuson, 2005). The anterior polarity of the EPI maintains the uncommitted state of EPI by the antagonizing signals of the WNT, BMP and NODAL signaling pathways from distal VE and extra-embryonic tissues (Arkell and Tam, 2012). Much have been studied on signaling factors and lineage specifiers in pre-gastrulation embryos, however, this dynamic process can augment differences in individual cells to generate various cell fates. In order to test the variation within single cell lineages, more and more advanced single-cell technologies (Kelsey et al., 2017), can provide a better understanding of cellular interactions, sensitivity to inter-cellular variation, and an evidence for heterogeneity in early mice post-implantation embryonic development, including germ cell lineage specification.

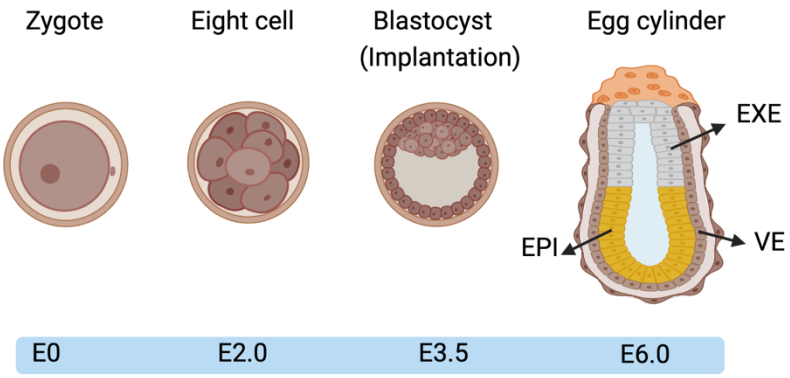

Fig.1 Illustration of mouse embryo development from fertilization to gastrulation. The morphological changes from fertilization (E0) to gastrulation (E6.0). VE, visceral endoderm; EPI, epiblast; EXE, extraembryonic ectoderm. E0, embryonic day 0; E2; embryonic day 2; E3.5, embryonic day 3.5; E6, embryonic day 6.

1.2 FORMATIVE PLURIPOTENCY WITH THE COMPETENCY FOR GERM CELL SPECIFICATION

Pluripotency can be divided into naïve and primed stages. These refer to pre- and post-implantation states in the mouse embryo *in vivo,* and are associated with embryonic stem cells (ESCs) and epiblast stem cells (EpiSCs) *in vitro* respectively. In mouse embryos, pluripotency arises within the ICM of the blastocyst and lasts 4-5 days until somatogenesis (Osorno et al., 2012). Upon implantation, EPI alters its cellular properties and undergoes a global transcriptomic and epigenomic change. This includes the expression of pluripotency related genes, DNA methylation, chimera development and the formation of germline specification. Formative pluripotency has been proposed as a stage between naïve pluripotency and primed pluripotency *in vivo* and *in vitro* (Smith, 2017). *In vitro*, epiblast-like cells (EpiLCs) are derived from ESCs during a 24–48-hour induction period in response to fibroblast growth factor (FGF) and activinA signaling. These cells resemble epiblast and have acquired the competence for germline induction. Formative epiblast have been hypothesized to act as a launching pad for multi-lineage differentiation; especially for the germline lineage (**Fig. 2A**), because naïve pluripotent cells (ESCs) must undergo a process of maturation before lineage decision. Meanwhile, primed cells (EpiSCs) are partially specified, and are cell fate biased. In our work, we have applied single cell RNA sequencing technology (Smart-seq2) (Picelli et al., 2014) to investigate the heterogeneity of epiblast cells, where the primordial germ cells (PGCs) are specified. We found that the epiblast cells of pregastrula embryos display three cell phases and we also captured transitions of pluripotency. This corresponds to the anterior, transition and posterior clusters in principal

component analysis (PCA) plot (**Fig.2B**) (Cheng et al., 2019). These three positional phases correspond to the pluripotency spectrum from naïve ESCs and primed EpiSCs (**Fig. 2C**).

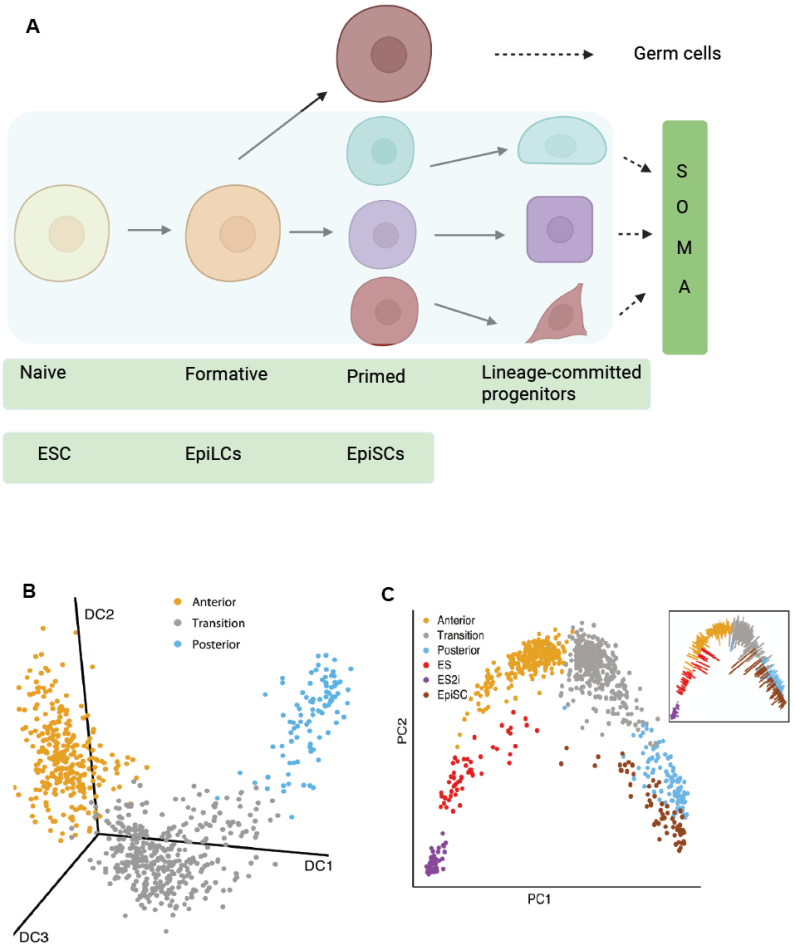

Fig.2 (A) Phased progression and heterogeneity model of pluripotency stage**.** Cells transit pluripotency from naïve stage to formative stage and further to primed stage along with lineage commitment. (B) Diffusion map demonstrating anterior, transition and posterior; three clusters of EPI cells. (C) PCA plot of EPI cells corresponding to ESCs and EpiSCs.

1.3 MOUSE GERM CELL SPECIFICATION

The requirement of the formative state is a link between germline lineage and somatic lineage specification of the pluripotent founders. At E6.25, the posterior part of epiblast segregates to a

group of competent founder cells as PGCs, in response to the signal from bone morphogenetic protein 4 (BMP4) secreted from surrounding extraembryonic ectoderm (EXE) tissues (Lawson et al., 1999).

The initiation of PGC specification involves the complex signaling crosstalk within the egg cylinder before gastrulation. BMP4, BMP4 antagonists, and an epiblast derived WNT3 signaling are involved in the process. Antagonists of BMP4 are secreted from the anterior visceral endoderm (AVE), inhibiting the anterior epiblast cells transform into germ cells. Moreover, in response to BMP4, the expression of *Wnt3* in the epiblast provides the competence for preparation of germ cell precursor fate (Rivera-Pérez and Magnuson, 2005). The signaling of WNT3 and BMP4 also activates the expression of transcription factor PR domain zinc-finger protein1 (*Prdm1*), PR domain zinc-finger protein 14 (*Prdm14*) and transcription factor AP-2 gamma (encoded by *Tfap2c*), all of which are crucial for germline specification (Ohinata et al., 2009).

The key repressors of somatic fates are crucial for germ cell specification. *Prdm1* also known as *Blimp1*, a transcriptional repressor and the earliest known marker of PGC fate that appears at E6.25 in a few pluripotent EPI cells, functions through repression of somatic mesodermal lineage. This is followed by upregulation of *Prdm14* and *AP2γ*, i.e. the other two key transcriptional factors during PGC specification (Ohinata et al., 2005; Yamaji et al., 2008).

*Wnt*3, acting as one of the earliest signaling genes, is expressed in the posterior VE and epiblast at around E5.75, which is known to activate primitive streak genes that are critical for gastrulation. It has been shown that some factors such as T (known as brachyury), one of WNT3's target genes, can be induced by WNT-β-catenin signaling during gastrulation to promote germ cell fate (Aramaki et al., 2013). We detected the expression of *Wnt3* in a discrete subset of EPI cells at E6.25 and E6.5 in the counterpart of transition and posterior phase (**Fig. 3**). Our discovery also provides an interesting clue to explore how WNT3 maintains and stabilizes the formative pluripotency that exits the naïve phase but maintains the competence for germ cell specification.

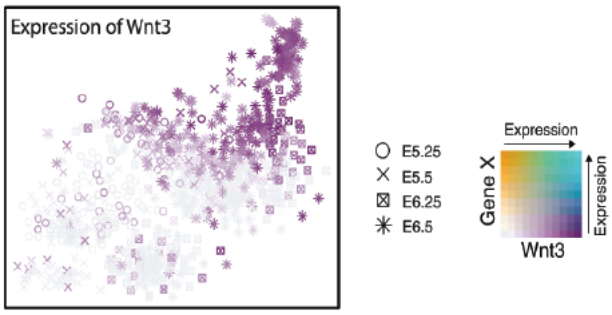

Fig. 3 *Wnt3* expression in the EPI cells.

1.4 GERM CELL MIGRATION

Germ cell migration is a complex and lengthy process which starts with the specification in epiblast and proceeds through different stages of migration, proliferation, apoptosis, epigenetic programming, sex differentiation and gametogenesis to ultimate formation of mature oocytes and spermatozoa. Therefore, each step following specification provides an opportunity for the emergence of heterogeneity. It is possible this is a selective step to make sure that the germ cells form the highest quality of adult gametes. PGCs migration is another crucial step to fulfill a reproductive competence. After PGC specification, the specified PGCs form a cluster of 30-40 cells at the base of the allantois at ~E7.25 far from their permanent tissue niche, which then later migrates along hindgut and colonizes the genital ridge at E10.5 (Saitou and Yamaji, 2012). It has been reported that stromal cell-derived factor 1 (SDF1) and the stem cell growth factor ligand (KITL) secretes from somatic cells, regulate PGC proliferation and survival while directing their movements (Gu et al., 2009). SDF1 binds to the chemokine receptor type 4 (CXCR4) on the leads them to migrate to the gonadal ridge. KITL binds to c-KIT on the PGCs and plays an important role in directing PGCs to gonadal ridge, whilst preventing apoptosis by promoting survival factors like NANOS3 and dead-end protein homolog 1 (DND1) during PGC migration (Molyneaux et al., 2003).

1.5 SEX DIFFERENTIATION

The next major differentiation event is sex differentiation. Shortly after a period of mitosis approximately at E12.5, germ cells are referred as oogonia and develop in clusters to form cysts while interacting with somatic cells in the ovary. The differentiation factors start to activate to produce female organs including *Sf1*, R-spondin-1, *Wnt4*, *Dax1*, and cytochrome P450, family 11, member A1 (*Cyp11a1*) (Chassot et al., 2014). *Wnt4* expression is increased, which inhibits the expression of *Cyp11a1,* delays steroidogenesis and increases the expression of female differentiation factors, *Follistatin* and *Dax1* (Yu et al., 2006). Oogonia begin to enter meiosis at about E13.5 and are then referred as oocytes. Oocytes proceed through the prophase I of meiosis to diplotene stages until arrested at E18.5, followed by cyst breakdown. Meiotic initiation is regulated by retinoic acid (RA), secreted by somatic cells in the mesonephros, which actives *Stra8* to promote meiosis of oocytes during early ovarian development (Anderson et al., 2008). Some oocytes undergo apoptosis after sex determination, and mouse oocytes clusters break down into single oocytes. A large number of oocytes are lost during the formation of primordial follicles (Pepling, 2006).

1.6 FOLLICLE DEVELOPMENT

Ovarian follicles are the main functional unit of the ovary, which houses oocytes and surrounding somatic cells including granulosa cells and theca cells. In mice, folliculogenesis is a carefully regulated and prolonged developmental process, starting with primordial follicle recruitment and ending in either ovulation or atresia. There are two phases during folliculogenesis: 1) the gonadotropin-independent phase which begins with activation of primordial follicles and ends with formation of small antral follicles and 2) the gonadotropin-dependent phase which involves a constant growth of small antral follicles to pre-ovulatory antral stage and ovulation (Ma et al., 2004).

Pituitary gonadotropins can influence early folliculogenesis during the gonadotropin-independent stage. However, this is not always the case as follicles can develop into antral follicles despite the lack of luteinizing hormone (LH) and follicle-stimulating hormone (FSH). Upon activation of the primordial follicle, communication between the oocyte and somatic cells enables the exchange of numerous regulatory signals that regulate oocyte metabolism, cell cycle progression and fertilization. Transforming growth factor-beta family cytokines (*Tgf-b*) is critical in regulating early folliculogenesis which serves as positive regulators to promote preantral follicle growth (Knight and Glister, 2006). On the other hand, the gonadotropin-dependent phase is closely regulated by hypothalamus-pituitary-gonadal (HPG) axis. Steroidal hormone also plays an important role in this process. Gonadotropin-releasing hormones (GnRH) from hypothalamus regulates FSH and LH secreted from anterior pituitary. The positive and negative HPG axis loops coordinate follicular maturation with sexual behavior and preparation for pregnancy. Estradiol is produced by developing follicles under the influence of FSH, which also inhibits LH production. However, when estradiol levels across a certain point - an LH surge is triggered. The oocyte's meiotic division is resumed as a result, and maturation starts before the oocyte is again arrested at MII stage (metaphase of second meiotic division). This oocyte is ovulated into the fallopian tube.

1.7 OOCYTE MATURATION

Mouse oocyte maturation is a tedious process to reach the competences for fertilization. Starting from the primordial follicle stage, the oocyte takes weeks to complete its growth, a 100-fold increase in size (Gougeon, 1996). During the maturation process, oocytes closely interact with

somatic cells, particularly granulosa cells. It has been found that metabolic cooperation, mediated by gap junctions and various cell-cell interactions, occurs between oocytes and somatic cells in the follicle to ensure sufficient substrate supplies to the developing oocytes (Li and Albertini, 2013). For example, oocyte-secreted factors like growth and differentiation factor 9 (GDF9) and bone morphogenetic protein 15 (BMP15) are directly involved in the modulation of energy metabolism, which are fundamental pathways that are lacking in oocytes but highly active in granulosa cells (Sugiura et al., 2005).

Moreover, paracrine signaling in oocyte maturation can stimulate preantral and antral follicles growth in many species, and androgens have been demonstrated as the most common steroid hormone in this setting (Emori and Sugiura, 2014). The action of androgens appears to be critical for normal follicle development and oocyte maturation. Androgens have also been shown to increase the granulosa cells' responsiveness to FSH for oocyte maturation (Laird et al., 2017). The androgen functions by binding the androgen receptor (AR) in the cell cytoplasm and then translocating the hormone-receptor complex to the nucleus, where it binds to a specific sequence in the target gene's promoter and promotes gene transcription (Askew et al., 2012). It has been reported that in AR knockout mice, there is significant disruption of hypothalamic regulation of gonadotropins, associated with abnormalities of ovary follicle development, and mice lacking AR showed reduced litter size (Walters et al., 2018a).

1.8 ANDROGENS AND POLYCYSTIC OVARY SYNDROME (PCOS)

PCOS is an endocrine disorder and the main cause of infertility in women worldwide, affecting ~15% of women of reproductive age. It is clinically characterized by hyperandrogenism, anovulation and polycystic ovarian morphology (PCOM). According to Rotterdam diagnostic criteria, at least two out of three features presented in the mentioned symptoms are diagnosed as PCOS (Dumesic et al., 2015). Hyperandrogenism is a key factor in the pathogenesis of PCOS, which is exhibited in more than 80% of women with PCOS, leading to increased production of ovarian theca cells and promoting early follicular growth that does not reach dominant stage and subsequent leads to ovulatory dysfunction (Rosenfield and Ehrmann, 2016). There is clear evidence showing there is an aberrant follicular development in women with PCOS. An increased number of preantral follicles and a higher proportion of primordial follicles have been activated in the ovaries of women with PCOS compared to control (Webber et al., 2003). The expression of a proliferation marker (*Mcm-2*) of preantral follicles has been shown to be increased in PCOS women (Stubbs et al., 2007).

Furthermore, about 75% of women with PCOS showed LH hypersecretion (McCartney et al., 2002). This is due to an increased pulsatile release of GnRH hormone from hypothalamus, leading to the elevated pulse frequency of LH by the pituitary gland. The neuroendocrine defect is thought to cause the increased ovarian theca cell production and ovarian hyperandrogenism and ovulatory dysfunction (Walters et al., 2018b).

Moreover, insulin resistance and hyperinsulinemia are exhibited in about 30% of women with PCOS (Cassar et al., 2016). Insulin enhances androgen production by stimulating the ovarian theca cells, and hyperinsulinemia in PCOS can elevate ovarian androgen production (Diamanti-Kandarakis and Dunaif, 2012). In addition, the sex hormone transporter, sex hormone binding globin (SHBG) is inhibited by hyperinsulinemia, which further contributes to hyperandrogenemia (Hammond, 2016).

1.9 ANDROGENS AND FETAL PROGRAMMING

The impact of excess androgen in animal models of PCOS indicates that exposure to excess androgen during fetal life may be as important as in adult life for the development of PCOS (Stener-Victorin et al., 2020). During pregnancy, the animals are given vast amounts of testosterone, which is enough to overload the buffering androgen action and cause fetus androgenization, mimicking many aspects of PCOS, including reproductive and metabolic dysfunction. This evidence provides the possibility that PCOS is a developmental disorder resulting from aberrant “programming” by excess androgen (Gorry et al., 2006).

Several PCOS-like mouse models have been created for fetal programming by uterus androgen exposure including the prenatal androgen (PNA) model, which is established by dihydrotestosterone (DHT) exposure to pregnant dams at gestational days between E16.5-18.5. The female first-generation offspring exhibit a disturbed estrous cycle with elevated testosterone and LH levels, and metabolic alterations in adulthood (Moore et al., 2015). In our study, to further explore the androgen effects on the most affected tissues by fetal programming, we transcriptomically profiled the key organs of F1 generation from the PNA mouse model. Furthermore, we used the PNA mouse model to investigate whether the maternal androgen excess environment can contribute to the inheritance of PCOS-like traits transgenerationally. The detailed findings are displayed in the result part as well as the publication.

1.10 ENVIRONMENTAL EFFECTS ON PCOS

There is growing evidence indicating that an adverse effect of maternal diet and hyperandrogenic exposure can manifest in further generations without further pathological exposure. The offspring across several generations have an increased propensity to develop metabolic, cardiovascular, and endocrine dysfunction. It has previously been reported that maternal high fat diet in mice increases both body size and insulin resistance till the second generation, and then almost vanishes in the F3 generation in females, suggesting an imprinting mechanism (Dunn and Bale, 2009). I and my colleagues have reported that daughters of mothers with PCOS are likely to be diagnosed with PCOS; this was also reported in a Swedish national cohort and a case control study from Chile (Risal et al., 2019). From our PCOS-like mouse model, the PNA mouse model, in which only F0 is treated with DHT, we have identified global gene expression alterations in the oocytes from F1-F3 female offspring. This is in line with transgenerational inheritance of PCOS-like phenotypes including reproductive and metabolic dysfunction. Next, we identified changes in the expression of genes that affected placental functions in F2 fetuses, suggesting that maternal uterine environment may play a great role in the process of affecting fetal life.

For a long time, it was well-known that parental lifestyle can influence offspring's development and these effects may last several generations. The mechanisms underlying this phenomenon remain unclear to this date. Recently, scientists have proposed epigenetics as an answer to this question. Epigenetic mechanisms such as DNA methylation and chromatin modification that can control gene expression, may be responsive to environmental perturbations. Adverse environmental exposure during sensitive developmental period can induce modifications in the epigenome of the embryo including the germline (Skinner et al., 2013). Therefore, alterations in the epigenome can cause heritable phenotypic changes that persist for several generations (Maccari et al., 2017). This phenomenon can be integrated into the hypothesis of the developmental origins of health and disease (DOHaD) (Barker, 1998), which seeks to explain why the period from conception to birth or the first years of life is important for determining lifelong susceptibility to non-communicable disease like diabetes mellitus and obesity. This sensitive period coincides the developmental timing which the germ cells are undergoing epigenetic programming. Thus, aberrant epigenetic remodeling in germ cells might potentially induce permanent modifications to the epigenome that are passed on to subsequent generations. This phenomenon is proposed as transgenerational epigenetic inheritance, which means exposure to an event in generation (F0) and the effect of this event must be observed in the third (F3) or fourth generation (F4). The mechanism underlying transgenerational epigenetic involves maintenance of DNA methylation, *de novo* methylation and small RNAs (Houri-Zeevi and Rechavi, 2017).

PGC specification leads to the greatest change of DNA methylation in fetal mouse germline. PGC specifies at E6.5 in the posterior epiblast, which are highly methylated as somatic cells but loses 90% of its global methylation in the following 7 days (Lee et al., 2014). In the fetal germline, demethylation occurs in two main states. The first starts at E8.0, during their migration to genital ridges (Seki et al., 2005). Bisulfite sequencing (Kobayashi et al2013) analysis suggested that the first demethylation is caused by inactivation of the maintenance methylation mechanism, which involves down-regulation of the expression of *Uhrf1* and removal of UHRF1 protein from nucleus. The passive demethylation diminished about 30% of global methylation levels when PGCs arrived at genital ridges (Kagiwada et al., 2013). Moreover, down-regulation of the *de novo* DNA methyltransferases DNMT3A, DNMT3B, and DNMT3L prevents restoration of methylation patterns during replication, contributing to a rapid loss during the first wave of demethylation (Kurimoto et al., 2008). Specific sequences include differentially methylated regions (DMR) in imprinted loci. Germline specific genes remain methylated despite a widespread reduction lasting until the second wave of demethylation. The second demethylation initiates at E11.5 once PGCs enters genital ridges. This process requires ten-eleven translocation proteins (TET): TET1 and TET2 proteins, which oxidized 5-methylcytosine (5mC) into 5-hydroxymethylcytosine (5hmC) (Vincent et al., 2013). 5hmC is further oxidized and replaced by base excision repair, whereas the passive pathway involves replication coupled dilution of 5mC under the absence or inhibition of maintenance DNA methyltransferase DNMT1 activity (Kagiwada et al., 2013).

In summary, epigenetic changes in the gene expression during early mammalian development occurs in response to adverse intrauterine exposure and can lead to heritable phenotypic changes that persist for several generations.

1.11 ANIMAL MODELS OF PCOS

In the past years, many PCOS-like animal models have been developed to study PCOS etiopathogenesis. The rodent models (mice and rats) are the most common (Stener-Victorin et al., 2020), because the insightful findings from customized animal models are often ways to gain a fundamental understanding of a human disorder. Rodents and humans share evolutionarily conserved similarities in the regulation of reproductive function by the hypothalamic-pituitary-gonad (HPG) axis and ovarian folliculogenesis.

Besides the maternal excess androgen exposure during fetal life (i.e., PNA), exposure to androgen in postnatal life also produces the metabolic and reproductive features of PCOS such as the peripubertal mouse model. The peripubertal androgenized mouse model is induced by continuous DHT exposure through a slow releasing pellet implanted subcutaneously from puberty presenting robust ovarian and cardiometabolic features mimic PCOS symptoms (Caldwell et al., 2014).

Altered sympathetic activity has been hypothesized in the development of PCOS. Increased expression of nerve growth factor (NGF) has been shown in women of PCOS ovaries (Dissen et al., 2009). It has been reported that women with PCOS have a 2-fold increase in NGF in the ovarian follicular fluid compared to their control, indicating the role of NGF in the PCOS pathology. In mice, excess ovarian NGF causes irregular cyclicity, compromised fertility, enhanced ovarian sex steroid production, and elevated granulosa cell apoptosis (Dissen et al., 2009). The genetically modified 17NF model overexpresses NGF in theca cells driven by 17α-hydroxylase promoter, leading to ovarian hyperandrogenism (Streiter et al., 2016). (Dissen et al., 2009). Moreover, these transgenic mice also display mildly elevated LH levels with increased testosterone production and metabolic dysfunction as reflected by impaired glucose metabolism and energy metabolism, aberrant adipose tissue morphology and function, and hepatic steatosis mirroring the PCOS pathophysiology. We have subsequently used the peripubertal androgenized mouse model and the 17NF mouse model to examine PCOS in adult programming in our study.

1.12 OBESITY MOUSE MODEL

PCOS is tightly linked to obesity, which is one of the important factors contributing to the development of PCOS. It has been shown that there are shared metabolic traits by large-scale genome-wide meta-analysis between PCOS and obesity (Day et al., 2018). Furthermore, the maternal obesity mouse model affects female germ cells and their offspring as well (Risal et al., 2019). Obesity and excess androgen may affect female fertility independently with distinct target as half of PCOS women are normal weight. Therefore, we include obesity mouse model to study the pathophysiology of lean PCOS and obese PCOS. In our study, we identified common transcriptome targets in hypothalamus, ovary adipose tissue and MII oocytes in the first-generation offspring of the maternal obesity mouse model and PCOS mice models. More detailed results can be found in the result section and manuscript III.

2 AIMS

Study I: To investigate cellular heterogeneity of pluripotency transition in epiblast and X chromosome dynamics during early mouse development.

Study II: To investigate whether maternal *in utero* exposure to androgens and/or maternal obesity leads to transgenerational transmission inheritance in adult female and to identify candidate genes that are involved in the transgenerational effects.

Study III: To define the molecular effects of fetal and adult programming by androgen in different PCOS-like mouse models as well as maternal obesity model.

3 MATERIALS AND METHODS

This part contains the main materials and methods used in this thesis. Detailed methodology can be found in the following publications.

3.1 ETHICAL CONSIDERATIONS

The Stockholm Ethical Committee for Animal Research granted permission to all animal experiments in study I to III (ethical permit numbers: study I: 2593-2607, study II: 10798-2017, study III: 20485-2020) in accordance with all applicable laws of the European Community and the European Parliament's 2010/63/EU directive on the protection of animals used in research. The regional ethical review committee, Stockholm, Sweden, granted its approval to the register-based study in study II (diary numbers 2013/862-31/5; 2016/1214-32).

3.2 SAMPLE COLLECTION AND ANIMAL MODELS

Study I:

Mouse embryos generated from mating between C57/BL/6J and CAST/EiJ mice were used for the first study. Table 2 shows single-cell samples from groups of embryos at different time points.

Day:	E5.25		E5.5		E6.25		E6.5	
Sex:	F	M	F	M	F	M	F	M
C57(F) x C57(M):	201/4	130/3	106/2	43/1	–	188/3	125/2	421/4
C57(F) x CAST(M):	–	–	38/2	82/2	97/2	36/1	–	–
CAST(F) x C57(M):	–	–	–	–	–	–	257/2	–
Total n cells:	331		269		321		803	
Total n embryos:	7		7		6		8	

Table 2 A summary table of single-cell samples from groups of embryos of different time points.

Study II:

Animal models:

Following a well-established protocol, the PNA model was generated by injecting 250 ug DHT dissolved in a solution (containing 5 uL benzyl benzoate and 95 uL sesame oil) to pregnant female mice from E16.5 to E18.5 (Moore et al., 2013; Witham et al., 2012). This model was used to mimic PCOS women in pregnancy with elevated levels of circulating androgen

(Glintborg et al., 2018; Sir-Petermann et al., 2002). The control mice were administered with 100 uL of the vehicle without DHT.

The PNA mice with maternal obesity were generated by the DHT treatment in combination with a high fat/high sucrose (HFHS) diet. The HFHS diet contained 58% fat, 26% carbohydrates, 17% sucrose and 16% proteins, whereas the control diet had 10 % fat, 73 % carbohydrate and 17 % protein.

To study the transgenerational effects of maternal androgen excess and maternal obesity in the offspring, we bred three generations of mice. The first generation (F1) was directly exposed to maternal lineage (F0) which was treated with DHT with/without the HFHS diet. The second generation (F2) was derived from PGCs of the F1 generation which were also directly exposed to the environmental excess androgen with/without the HFHS diet. The third generation (F3) was derived from the F2 generation and was indirectly exposed to environment excess androgen with/without the HFHS diet.

Study III:

Animal models:

We used four animal models of PCOS as well as an obesity mice model in study III to investigate the fetal programming (F1 generation) due to the maternal effect and the adult programming of PCOS. The fetal programming mice models comprised of the PNA mice model and the HFHS mice model mentioned in Paper II. The adult programming study comprised of two animal models: the peripubertal androgenized mice model and the 17NF mice model.

The peripubertal androgenized mice model was generated by continuous exposure to a 10 mm DHT pellet from pubertal period and onwards. This model was generated to mimic PCOS with reproductive and metabolic phenotypes. At 4 weeks of age, the female mice were given an implant containing a 10 mm DHT pellet or a control pellet (for the control group) and exposed for 7 weeks.

A transgenic mice model of PCOS referred to as 17NF was also used in this paper (Dissen et al., 2009). The 17NF mice carry a transgene that expresses NGF under the control of the 17alpha-hydroxylase gene promoter. Thus, NGF is overexpressed in the theca cells of the ovary in these animals. The 17NF mice were generated to mimic PCOS-like symptoms including reproductive and metabolic phenotypes and were bred to homozygosity. To be comparable, B6background mice were used as the control group.

3.3 EXPERIMENTAL STUDY

3.3.1 Single-cell sample preparation from early-stage embryos

First, the embryos were dissected from decidua and were washed with DMEM medium twice. TrypLE was used to dissociate embryos into single cells for 15 minutes, then a mouth pipette was used to manually pick single cells. The picked single cells were collected into PCR tubes with Smart-seq2 lysis buffer.

3.3.2 Sample collection of MII oocytes, embryos and organs

In study II and study III, mice were fasted for 2 hours before the collection of oocytes, embryonic tissues and organs. In study II, embryonic tissue (placenta) and organs (liver, subcutaneous adipose tissue) were dissected from F1, F2 and F3 female mice, and the embryos were collected at E12.5, and E18.5 of F2 generation in androgenized lineage and obese lineage. In study III, subcutaneous adipose tissue, ovaries, and hypothalamus were collected from the PNA model, the peripubertal androgenized mice model, the 17NF mice model as well as the maternal obesity mice model. The tissues were quickly dissected on ice, snap froze in liquid nitrogen and then stored at -80°C.

In study II and study III, the MII oocytes from the PNA (F1 generation, F2 generation and F3 generation of female offspring), peripubertal androgenized, 17NF and maternal obesity mouse models were collected from 20-week-old female mice. To superovulate these mice, they were given an injection of 5 IU (international unit) of pregnant mare's serum gonadotropin (PMSG) and 5 IU of human chorionic gonadotropin (hCG) after 48 hours. The Cumulus-oocyte complexes were then dissected out from the oviduct ampulla, 16 hours after hCG injection. The single MII oocytes were isolated from the complexes and rinsed with M2 medium.

3.3.3 RNA extraction and mRNA expression analysis

Mice embryonic tissue and mice organ tissue (liver, placenta, subcutaneous adipose tissue, hypothalamus, and ovary) were homogenized in 1 mL TRI reagent. Total RNA was extracted following manufacturer's instructions. The eluted RNA was treated with DNaseI to remove DNAs. A small amount (500 ng) of total RNA was used to synthesize cDNA. Quantitative real-time PCR was performed using SYBR Green PCR Master Mix for relative gene expression analysis. A housekeeping gene *Gapdh* was used to normalize the expression of target genes.

3.3.4 3.4.4 Bulk RNA sequencing library preparation

Total RNAs were isolated from mouse subcutaneous adipose tissue, hypothalamus and ovary. For bulk RNA sequencing, 1 ng of total RNA was used for sequencing library construction. Smart-seq3 protocol was used to generate sequencing libraries (Hagemann-Jensen et al., 2020). Briefly, messenger RNAs (mRNAs) were reversed transcribed by Maxima H-minus reverse transcriptase. The second strand cDNAs were synthesized by a template-switching reaction followed by 12 cycles of PCR amplification using KAPA HIFI Hot-Start polymerase (Roche). The cDNAs were cleaned up using 22% PEG beads (Sigma Aldrich) and quality checked using BioAnalyzer 2100 (Agilent Technologies). Then, 200 pg of cDNA was used for tagmentation by Tn5 transposase (Illumina) and followed by 10 cycles of PCR amplification.

3.3.5 Single-cell sequencing library preparation from early mouse embryos

The cDNA library was prepared using Smart-seq2 protocol (Picelli et al., 2014). mRNAs were reverse transcribed using SuperScript II enzyme after cell lysis. Template switching reaction was utilizing for second-strand synthesis. cDNA amplification was prepared by 18 cycles of PCR reaction using KAPA HIFI HotStart ReadyMix. cDNA libraries were then cleaned up using 22% PEG beads and quality checked using BioAnalyzer. Sequencing libraries were generated by tagmentation of 1 ng cDNA using Tn5 transposase followed by 8 cycles of PCR amplification.

3.3.6 Sequencing library preparation of MII oocytes from PNA model, maternal obesity model and 17NF model

cDNA library was prepared using Smart-seq2 protocol as mentioned before. mRNAs were reverse transcribed by SuperScript II reverse transcriptase after cell lysis. Template switching reaction was used to synthesize second-strand cDNAs. cDNA amplification was performed with 14 cycles of PCR reaction using KAPA HIFI HotStart ReadyMix. cDNA libraries were then cleaned up using 22% PEG beads and quality checked using BioAnalyzer. Sequencing libraries were generated by tagmentation of 1ng cDNA using Tn5 transposase followed by 8 cycles of PCR amplification.

3.3.7 Sequencing library preparation of MII oocytes from Peripubertal model

cDNA library was generated using Smart-seq3 protocol. Following by cell lysis, mRNAs were reverse transcribed using Maxima H-minus reverse transcriptase. The second strand for cDNA amplification was conducted by a template-switching reaction followed by 14 cycles PCR by KAPA HIFI Hot-Start polymerase (Roche). The cDNA was cleaned using 22% PEG beads and quality checked using BioAnalyzer (Agilent Technologies). Then, 200 pg cDNA was tagmented with Tn5 transposase (Illumina) followed by 10 cycles of PCR amplification.

3.4 BIOINFORMATICS AND STATISTICAL ANALYSIS

3.4.1 RNA sequencing data processing for early mouse embryonic sample

Raw reads were mapped to the mouse reference genome (GRCm38/mm10) by STAR with default parameters. Cells of low quality (less than 5000 expressed genes) and lower mapping ratios (less than 70%) were excluded.

3.4.2 RNA sequencing data processing and quality control for MII oocytes

Mouse reference genome (GRCm38/mm10) was used to align the raw reads by STAR with default parameters. For the samples constructed by Smart-seq3 protocol, zUMIs (Parekh et al., 2018) pipeline was applied for mapping process. Cells of low qualities (fewer than 3000 expressed features) and lower mapping reads (less than 200,000) were excluded.

3.4.3 Bulk RNA sequencing data processing and quality control

Raw reads were mapped to the mouse reference genome (GRCm38/mm10) by STAR with default parameters. zUMIs (Parekh et al., 2018) pipeline was applied for mapping process. Cells of low complexity (fewer than 5000 expressed genes) and lower mapping reads (less than 20,000) were excluded.

3.4.4 Data Normalization and batch effect correction for MII oocyte

Seurat normalization method ‘LogNormalize’ was used to normalize three generations of MII oocytes from the PNA and the maternal obesity model. Then the Seurat ‘ScaleData’ function was applied to remove the batch effect due to technical variations.

3.4.5 Differential gene expression analysis and Gene Ontology analysis

The differential gene expression analysis was calculated after removing batch effect and the read counts were analyzed by ‘DESeq2’ R package. Differential expressed genes (DEGs) were defined by $p < 0.05$ and the absolute value of log2 foldchange over 0.5. Ontology analysis of DEGs were conducted by ‘Clusterprofiler’ R package.

3.4.6 Pseudospace analysis in EPI cells

In order to identify subclusters, a diffusion map was used to analyze the EPI cells. Counts were normalized by estimateSizeFactorMatrix function from ‘DESeq2’ R package, and then the top variable genes were used for separating the EPI cells into three-dimensional space at the diffusion map ($k = 3$). Further, principal curve was calculated by ‘princurve’ R package based on the first two dimensions. The pseudospace cell trajectory was obtained based on the projected coordinated on the first dimension of the diffusion map.

3.4.7 Weighted gene co-expression network (WGCNA) analysis

Data were analyzed by ‘WGCNA’ R package (Zhang and Horvath, 2005). The power parameter with soft threshold of 9 was selected by ‘pickSoftThreshold’ function. The Pearson correlation was used in the analysis and the correlation between module eigengenes and different treatments of mice models were calculated to identify modules of interest which were significantly associated with the treatments of mice models.

3.4.8 Cell-Cell communication analysis

To investigate cell-cell communication between MII oocytes and other ovarian cells, ‘CellChat’ R package (Jin et al., 2021) was used to analysis the ligands and receptors between the cells. Ligand-receptor pairs were defined based on ‘CellChatDB’ database. Based on

biological function, all the interactions were grouped into 229 signaling pathway families. The differentially expressed signaling genes were identified by Wilcoxon rank sum test with significance level of 0.05.

3.4.9 Metabolic pathway analysis of MII oocyte

Metabolic pathway quantification in MII oocytes was conducted by 'scMetabolism' R package (Wu et al., 2022). The function AUCell was used to quantify the metabolic activity after implementing the Seurat pipeline. The genes for pathway analysis can be found online (https://github.com/wu-yc/scMetabolism).

3.4.10 Statistical analysis

In the cohort study in study II, correlations between maternal PCOS and daughters diagnosed with PCOS were calculated by stratified Cox regression models with hazard rations of 95% confidence intervals. Potential confounding variables were adjusted in the model according to daughter's year of birth, maternal education, maternal region of birth and maternal age at daughter's birth. The statistical analysis in case-control study in study II were conducted using GraphPad Prism. The detailed descriptions of statistical analysis can be found in the Method section of the respective publications.

4 RESULTS

This part summaries the main findings of the three studies included in the thesis. More detailed information can be found in the respective publications.

4.1 STUDY I:

4.1.1 Transcriptome profiling of 1,724 single cells from pregastrula embryos

Next-generation sequencing (NGS), especially single-cell RNA sequencing, is a powerful tool for investigating the intracellular transcriptomes on embryogenesis. In this study, we have sequenced over 2000 single cells to reconstruct the developmental trajectory from pregrastrua embryos from E5.25 to E6.5 four time points. Three major clusters were found, which were annotated as EPI (*Pou5f1*), VE (*Amn*) and EXE (*Bmp4*) according to their marker genes (**Fig 4**). As we detected, *Wnt3* expression was highly expressed at E6.25 and E6.5 of EPI cells with positive correlation of primitive streak markers including *T*, *Mixl1,* and *Eomes*, and with negative correlation of pluripotency markers like *Dppa4*. These results indicate the heterogeneity of EPI cells.

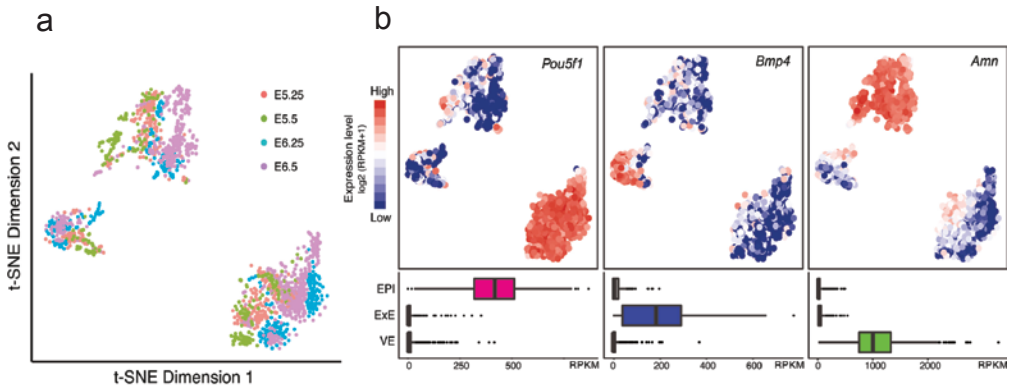

Fig 4 Transcriptome profiling of 1,724 single cells (a), t-SNE plot of pregrastrua embryos from E5.25 to E6.5. **(b),** Expression of lineage marker genes presented in t-SNE plot; EPI lineage marker: *Pou5f1*; EXE lineage marker: *Bmp4*; and VE lineage marker: *Amn*.

4.1.2 Heterogeneity of EPI cells with spatial trajectory

To further investigate the heterogeneous fates of EPI cells, we applied a 3D diffusion map to reconstruct the developmental trajectory of the EPI cells. We identified three clusters of EPI cells and designated the three clusters as anterior, posterior and transition state which is an intermediate state with co-expression of both anterior and posterior related genes (**Fig 5a and 5b**). To refine the resolution of spatial allocation of individual EPI cells, we assigned the EPI cells from a 3D dimensional pseudo-space trajectory onto a 2D dimensional pseudo-space trajectory based on principal curve (**Fig 5c**). Then we compared the transcriptome the anterior, posterior and transition states using naïve pluripotency cells ESC cells, primed pluripotency cells EpiSCs and intermediate pluripotency cells EpiLCs. We found that EPI cells of three states covered from naïve to primed pluripotency (**Fig 5c**).

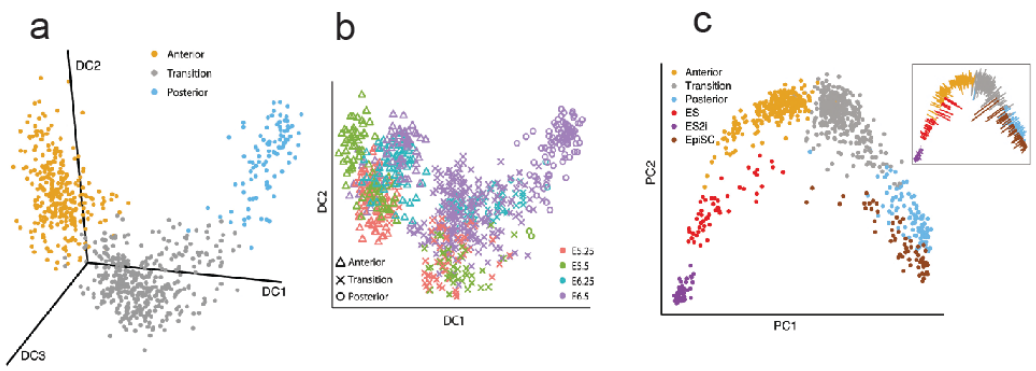

Fig 5 Spatial trajectory in EPI lineage. (a), Three clusters (anterior, posterior and transition) presented in 3D diffusion map. **(b),** Cells in three states (anterior, posterior and transition) annotated by embryonic age. **(c),** PCA plot of EPI cells and ES2i, ESC, EpiLCs, and EpiSCs fitted onto principal curve.

4.1.3 The dynamics of XCI and XCR in early mouse embryonic development

To understand the dynamics of XCI and XCR in EPI, VE and EXE lineage, we calculated the expression of allele-specific X-linked genes. We found in female cells that the expression of the X-linked genes presented significantly different in EPI lineages with 74.5% of reads and EXE lineages with 85.4% of reads, indicating XCR initiates in EPI lineages (**Fig 6a and 6b**). In EPI lineages, at E5.5, we discovered that the expression of Xp and Xm alleles are almost equally expressed. XCR reversed the silencing of Xp was entirely established in EPI lineages, and most EPI cells completed random XCl by E6.5.

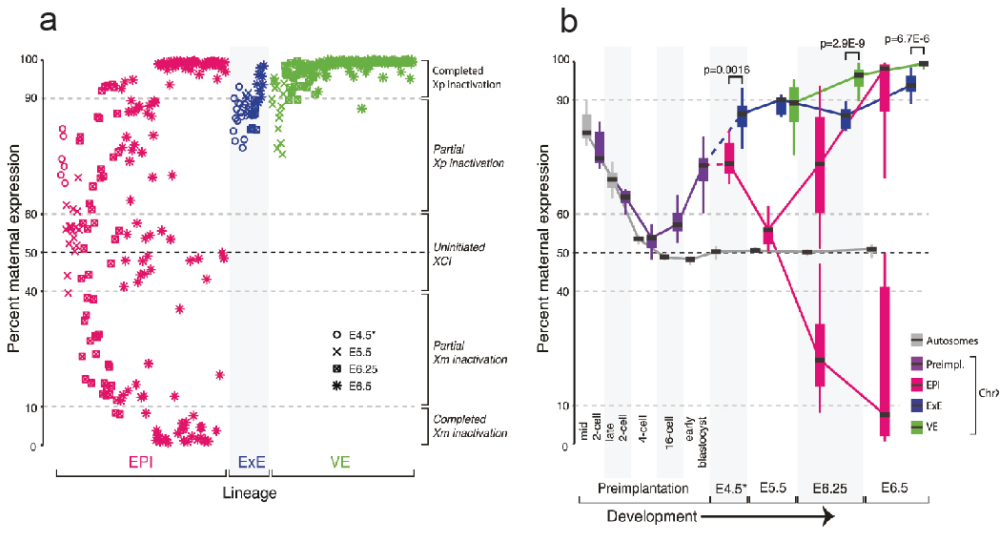

Fig 6 Dynamics of XCl and XCR. (a), Percentage of gene expression of Xm in EPI, VE and EXE at different time points**. (b),** Percentage of gene expression of Xm and autosome in developmental timeline in EPI, EXE and VE lineage was presented in boxplot.

4.1.4 Conclusion

Our study provides a detailed transcriptional analysis of post-implantation embryonic development. We captured three states of EPI cells (anterior, transition and posterior) along pluripotency continuum and we studied the dynamic X chromosome activity in gastrula embryos. Our results provide a valuable resource to develop the methodology *in vitro* to maintain the formative pluripotency.

4.2 STUDY II:

4.2.1 Swedish national cohort study

A Swedish national wide register-based study indicated that there is an increased risk of daughters of women with PCOS diagnosed of PCOS compared to daughters born to women without PCOS. Seventy-one percentage of daughters of women with PCOS met the Rotterdam criteria for diagnosis of PCOS in the longitudinal study.

4.2.2 Prenatal androgen exposure causes transgenerational reproductive and metabolic dysfunction in offspring

We explored that F2 generation of androgenized lineage has smaller embryo size at E12.5 and E18.5 compared to the control group. We further analyzed the expression of genes (*Tfap2c, Akt1, Ascl2*) that affect placenta function, showing a decreased gene expression level at E12.5 in androgenized lineage. And female offspring of F1, F2 and F3 had longer anogenital distance than controls in androgenized lineage. These results indicate that prenatal androgen exposure causes transgenerational reproductive dysfunction.

We found that female offspring of F1 and F3 had increased fat mass and F1-F3 female offspring in androgenized lineage showed a larger adipose size with altered gene expression affecting adipogenesis and lipid biosynthesis. We also discovered that F1 and F3 female offspring displayed impaired energy balance in the androgenized and obese lineages. Taken together, these results suggest that prenatal androgen exposure leads to transgenerational metabolic dysfunction.

4.2.3 Transcriptome profile of MII oocytes from F1 generation to F3 generation

To further explore fetal reprogramming through maternal germline, we did transcriptome profile of the female offspring of MII oocytes from F1 generation to F3 generation androgenized lineage and obesity lineage. We found 410 DEGs in androgenized lineage and 231 DEGs obese lineage respectively (**Fig 7a**). Then we annotated these DEGs with biological ontology analysis. The top biological enrichment terms of germ cell and reproductive process, steroid hormone signaling pathways and glucose homeostasis were involved in androgenized lineage, whereas several metabolic processes such as energy metabolites, ATP metabolic

process and mitochondrial transport signaling pathways were involved in obese lineage. (**Fig 7b and 7c**).

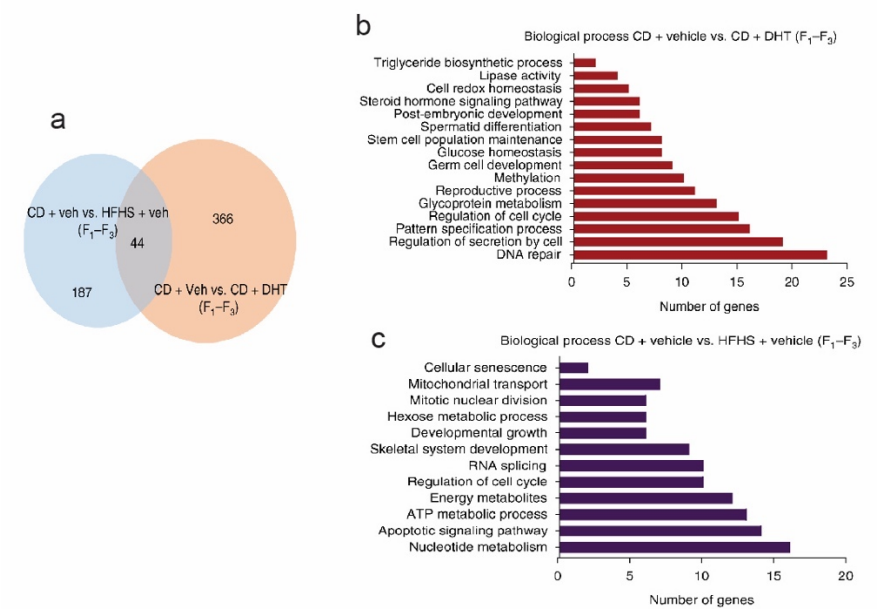

Fig 7 (a), DEGs of MII oocytes from F1 to F3 generations in androgenized lineage and obese lineage displayed in Venn diagram. **(b),** GO enrichment terms in androgenized lineage. **(c),** GO enrichment terms in obese lineages.

4.2.4 Common gene signatures in serum of daughters from women with PCOS

We first compared our DEGs of MII oocyte with the DEGs in subcutaneous adipose tissue of women with PCOS in previous study. We found 33 DEGs in androgenized lineage and 23 DEGs of MII in obese lineage which overlapped with human adipose tissues (**Fig 8a**). Many genes in androgenized lineage such as *Pogz, Tmem214, Rhoa, Tial1* are involved in embryonic development. We examined the DEGs in human serum samples from daughters of women with and without PCOS from Chile as well as the serum sample from women with PCOS or without PCOS. Our result showed that FABP5 increased expression in human serum, whereas the expression of *RNF141*, *INTS3* and *INIP* were downregulated, similarly to gene expression profile of MII oocytes in androgenized lineage (**Fig 8b**).

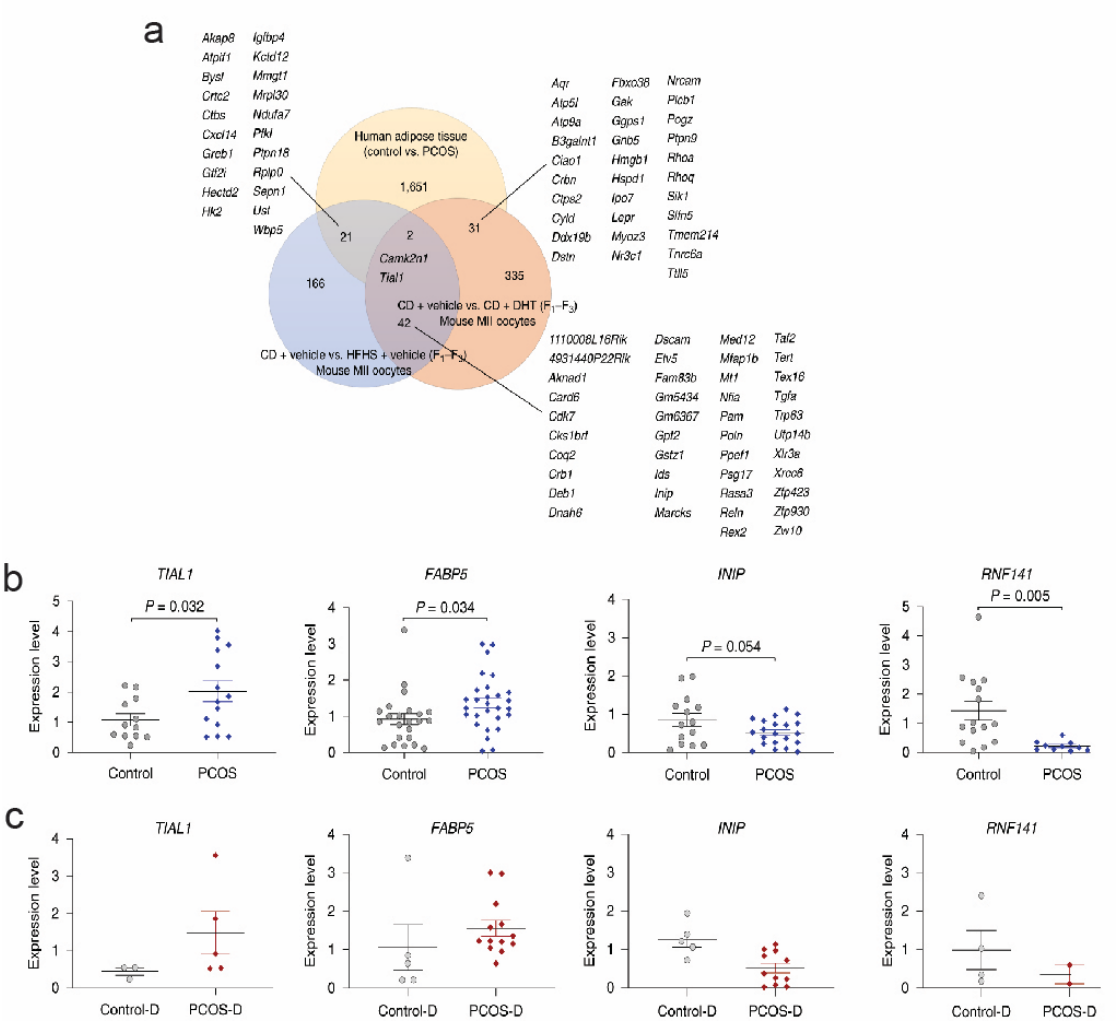

Fig 8 (a), Overlapping DEGs of MII oocyte in androgenized lineage and obese lineage human adipose tissues. **(b,c)** mRNA expression level of *TIAL1*, *FABP5*, *INIP*, and *RNF141* in serum of women with PCOS and daughters of women with PCOS.

4.2.5 Conclusion

Our results of transgenerational effects in the PNA mouse model and the maternal obesity mouse model suggest that there is a strong adverse effect of androgen excess during the gestation stage. These transgenerational consequences are exhibited in both metabolic and reproductive dysfunctions, which are mediated by environmental androgen excess *in utero* and oocyte-derived factors. By comparing human and mouse tissue, we found common

transcriptional signature, suggesting that transgenerational effects can be evaluated in different tissues.

4.3 STUDY III:

4.3.1 Transcriptome profile of hypothalamus, ovary and adipose tissue in PCOS-like mouse model and obesity mouse model

In order to investigate the fetal and adult reprogramming in PCOS-like mouse models as well as the effects of maternal obesity, we performed transcriptome profile of key target tissues in those animal models. We found the greatest number of DEGs in the PNA model compared to the others in hypothalamus, suggesting fetal programming effects. As chronic anovulation is one of the hallmarks of women with PCOS and irregular estrous cycle is one of the most prominent phenotypes in these PCOS-like mouse models. We identified several common and unique DEGs of different animal models in the ovaries that might lead to ovarian phenotypes. By comparing those DEGs in different animal models, we performed gene ontology (GO) enrichment analysis. We identified common pathways like the ERK1 and ERK2 pathways, the ovarian follicle development pathway (shared by the PNA and the peripubertal androgenized model) and the unique pathways in PNA such as placenta development and maternal behavior in the peripubertal androgenized model.

Obesity is a common feature in women with PCOS and adipose tissue dysfunction is likely involved in the development of PCOS and associated metabolic disturbances. Our animal models have shown increased fat mass and enlarged adipocytes. By transcriptome profile of adipose tissue in different mice models, we identified the largest number of DEGs (1910) in the peripubertal androgenized model, suggesting potential adult programming of DHT in adipose tissue. Next, we compared the biological function of those DEGs in different animal models. Lipids, glucose and regulation of inflammatory response was enriched in all models, whereas the testosterone response was enriched in the PNA, the peripubertal androgenized model and the obese model. Our finding suggests that adipose tissue is largely affected. We then performed correlation analyses between the DEGs in each animal model and the DEGs in the adipose tissue of women with PCOS (Divoux et al., 2022)，and we found strong correlation between each model and women with PCOS. We discovered that *Ms4a6e* is common to all PCOS-like models, also with high fold change in expression in adipose tissue of women with PCOS.

4.3.2 Transcriptome profile of MII oocytes and cell-cell communication between ovary and MII oocyte in each mouse model

We perform transcriptomic profile of MII oocytes, to understand how different windows of androgen and maternal obesity exposure affects MII oocytes mouse models. We detected the most DEGs were in the 17NF model, suggesting that the genetic modification of granulosa cells greatly affects the oocytes. GO annotation enrichment analysis revealed that there were several pathways involved in all animal models: namely glucose metabolic process, insulin response and meiotic cell cycle. Several unique pathways were found in the 17NF model – namely ovarian follicle formation pathway, the steroid pathway and ERBB signaling pathway.

As androgens stimulate the growth of preantral and antral follicles, and impair follicle maturation, to explore the communication between MII oocytes and surrounding follicular niche by androgen, we conducted cell-cell communication by ligand-receptor analysis. We identified several distinguished signaling pathways in each animal model. We found that the BMP signaling pathway, the KIT signaling pathway, the Adiponectin signaling pathway, the EGF signaling pathway, the IGF singling pathway and the insulin signaling pathway were affected by androgen and maternal obesity exposure.

4.3.3 Fetal and adult androgen exposure modulates metabolic pathways in MII oocytes

Because emerging evidence indicates that metabolism is a major determinant of oocyte quality, we investigated whether any metabolic changes affect MII oocyte quality in our animal models. We quantified the metabolism activity of MII oocytes, and we found unique metabolic changes in PCOS-like and maternal obesity mouse model. Peptide hormone metabolism is affected in the PNA model (**Fig 9a**); glucose metabolism is significantly decreased in the maternal obesity model (**Fig 9b**); steroid hormone homeostasis is significantly decreased in the peripubertal androgenized model (**Fig 9c**) and oxidative phosphorylation metabolism pathway is significantly upregulated in the 17NF mouse model (**Fig 9d**).

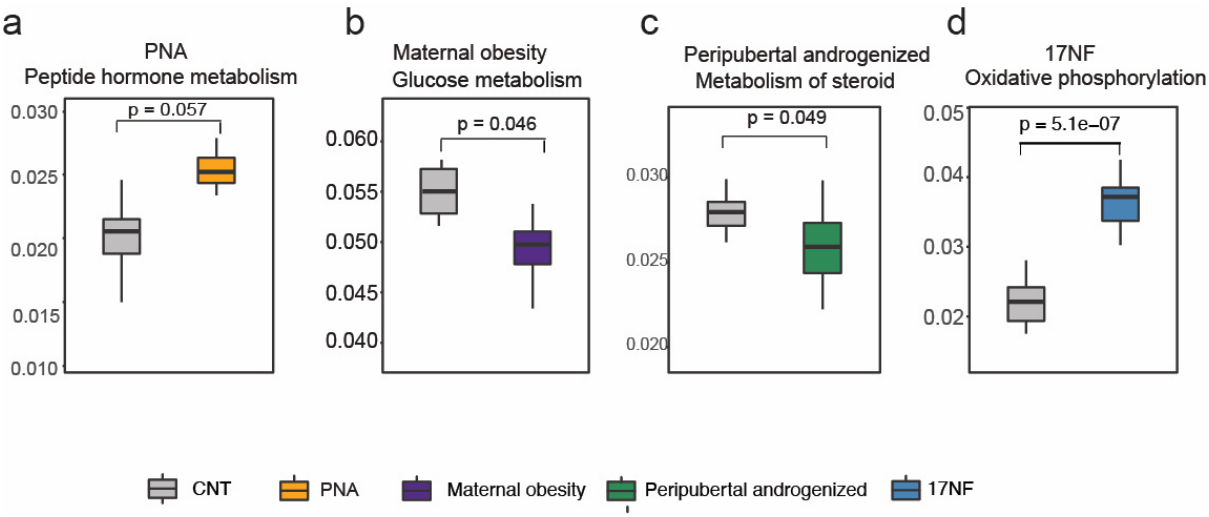

Fig 9 (a-d) Significant metabolic pathways in PNA, Maternal obesity, Peripubertal androgenized and 17NF mice model respectively.

4.3.4 Conclusion

Our study provides a comprehensive transcriptomic profile of key target tissues in the PCOS-like animal model and the maternal obesity model, which is a unique resource for the research community. Several common functional pathways are identified across all the animal models despite of different gene targets. Ovary and adipose tissue are more affected than the hypothalamus in the peripubertal androgenized model, the 17NF model and the maternal obesity mouse model. Fetal programming exerts a strong effect on hypothalamic gene expression, especially in the PNA mouse model. The adipose tissue of the peripubertal androgenized model was the most affected, which was in line with the phenotype of this model.

5 DISCUSSION AND FUTURE PERSPECTIVE

In this thesis, we applied single-cell RNA sequencing to study the pregastra embryos' development as single cell RNA sequencing technology is a useful tool to elucidate the dynamics of molecular regulation of lineage differentiation and particular cell type in a heterogeneous population. Moreover, single-cell RNA sequencing analysis allows us to reconstruct the cell-lineage trajectories and the cell state transition.

In study I, we found that EPI cells displayed three cell states (anterior, posterior and transition) along the pluripotency continuum which correlate the pluripotency spectrum from naïve ESCs to primed EpiSC. Our findings indicate that the epiblast of pregastra embryos undergo pluripotency transition and could represent the counterpart of formative pluripotency *in vivo*. According to Smith *et al*, naïve pluripotent cells need to go through a maturation process for lineage decision and the primed cells have already partially determined (Smith, 2017). Thus, the formative state between the naïve state and the primed state is important for obtaining the competence of lineage decision and germ cell fate. We captured formative pluripotency which can serve as an improved point for guiding the differentiation to germline, as germline competence is acquired in the formative pluripotency between the naïve and the primed states.

Meanwhile, we explored the expression of *Wnt3* in EPI cells which maintain and stabilize the formative pluripotency that exits the naïve pluripotency but remains competent for germ cell specification. Our finding provides an interesting clue to explore whether Wnt3 signaling can stabilize the transient competence for PGCLC induction *in vitro*. Our current study applied GSK inhibitors (CHIR99021) that actives WNT signaling pathway to maintain formative pluripotency *in vitro*. We proved that WNT signaling sustains naïve gene expressions as a counter force of differentiation induced by FGF2 and activinA.

In study II, we studied whether environmental factors (maternal androgen excess and maternal obesity) could contribute to the onset of the disease and whether the PCOS phenotype could be transgenerationally transmission inherited in female offspring. Our findings provide the evidence that maternal androgen excess can initiate the PCOS-like phenotype in the offspring spanning multiple generations. Metabolic dysfunction in androgenized lineage including increased fat mass, larger adipocytes, higher liver triglyceride concentration and larger lipid droplets can be transgenerationally transmitted, which is in line with previous clinical studies in humans (Petta et al., 2017).

The cause of transgenerational inheritance of PCOS might be genetic and epigenetic modifications to the germline. Oocytes needed for early embryo development can have long-lasting effects on the progeny and potency of future generations. Our sequencing result of MII oocytes showed the altered gene expression across generations, suggesting prenatal androgen exposure has more adverse and long-lasting effects on oocyte function.

Future research can focus on the molecular mechanisms that leads to these phenotypes such as the milder effect on F2 generations. Moreover, we might apply a multi-sequencing method to understand the genetics and epigenetics underlying the transgenerational effects.

In study III, we performed transcriptomic mapping of key target tissues among different PCOS-like mouse models. Although there are several mouse models that has well characterized PCOS features, no comprehensive transcriptomic profiling at the molecular level across key reproductive and metabolic tissues has been done to this date. We compared common and unique molecular features in the hypothalamus, ovary, subcutaneous adipose tissue and MII oocytes in order to define the molecular effects of fetal and adult programming by the administration of androgen in the PCOS-like mouse model and the maternal obesity model. We show that fetal programming exhibits a strong effect on the hypothalamic gene expression compared with adult programming. This suggests that the altered regulation of hypothalamus-pituitary-gonad (HPG) axis might contribute to the PCOS phenotype. By comparing the cell-cell communication between oocytes and the ovary, we found several common and unique signaling pathways driven by androgen exposure and maternal obesity. Our studies of transcriptomic profiling of multiple organs might provide the novel knowledge about their interactions and help to identify common affected pathways to understand the pathology and possible treatments of PCOS. It's possible that our findings are directly transferable to the study of humans, but this remains to be investigated in future studies.

6 ACKNOWLEDGEMENTS

It has been a great journey to complete my doctoral study in Qiaolin Deng's group at the Department of Physiology and Pharmacology in Karolinska Institutet. I enjoy these last few years in Stockholm with sweet and sometimes bitter memories. I want to thank those beautiful people who helped and supported me during these years.

I must first thank my main supervisor **Qiaolin Deng**. I want to thank you for leading me into the trip at this wonderful university. I want to thank you for always trusting me and supporting me at any time. Thank you for your inspiration and guidance, that will be my lifelong treasure.

Another very important person in my academic life is my co-supervisor **Daniel Ramsköld**. A big thank for all your support and help. Whenever I need help, you are always there. I really appreciate having you as my co-supervisor.

I would like to thank my co-supervisor **Elisabet Stener-Victorin.** It's an honor to have you as my co-supervisor. Thank you for guiding me in the PCOS journey. I learned a lot during many collaboration projects. I would like to thank my co-supervisor **Johan Ericson.** Without you I could not start this wonderful journey.

Special thanks to my mentor **Hong Jin**, my elder sister in Christ. Thank you for your love and support.

I would like to thank the great people I have met in Deng's lab. Present (**Han, Qing, Wenteng, Hong, Allan, Emilie, Sanjiv, Ran**) and former (**Julio, Ou, Ahmed**) team members, thank you for all the great moments we had, all the help and knowledge sharing. I would like to give extra thanks to **Qing, Han, Hong**, for being great friends and colleagues.

I would like to thank people in Elisabet's lab. **Haojiang, Congru, Gustaw, Eva, Sanjiv, Sara, Angelo**, thank you for the great times we had.

Thanks to my dear friends, **Lianhe, Wenyu, Yanan, Marika**, for the great company and moments we had. **Chikai**, thank you for the great help.

I want to express my gratitude to my friends and Christian sisters, especially **Jingwen** and **Dan**, thank you for all the support and caring. Thank you, all good fellows, **Peiyao, Bing, Aiping, Haitang, Sunny and Yafeng**.

To **Michael** and **Christoph**, thank you for the great help.

Thanks to all my friends and colleagues at KI or out of KI:

Quan, Tenghao, Zelong, Yunbing, Shuijie, Huaitao, Zhengbing, Shengduo, Ping, JinMing, Zijian, Juan, Shanshan, Wei, Lipeng, Shuangyang, Naify, Maribel, Per, Gert-Jan, Mtakai, Per, Leo, Yachao, Anton and Petra.

To **my boyfriend**, thank you for your love, support and care.

To **my family**, thank you for your endless love and full support!

7 REFERENCES

Anderson, E.L., Baltus, A.E., Roepers-Gajadien, H.L., Hassold, T.J., de Rooij, D.G., van Pelt, A.M.M., and Page, D.C. (2008). Stra8 and its inducer, retinoic acid, regulate meiotic initiation in both spermatogenesis and oogenesis in mice. Proc. Natl. Acad. Sci. U. S. A. *105*, 14976–14980. https://doi.org/10.1073/pnas.0807297105.

Aramaki, S., Hayashi, K., Kurimoto, K., Ohta, H., Yabuta, Y., Iwanari, H., Mochizuki, Y., Hamakubo, T., Kato, Y., Shirahige, K., et al. (2013). A mesodermal factor, T, specifies mouse germ cell fate by directly activating germline determinants. Dev. Cell *27*, 516–529. https://doi.org/10.1016/j.devcel.2013.11.001.

Arkell, R.M., and Tam, P.P.L. (2012). Initiating head development in mouse embryos: integrating signalling and transcriptional activity. Open Biol. *2*, 120030. https://doi.org/10.1098/rsob.120030.

Askew, E.B., Minges, J.T., Hnat, A.T., and Wilson, E.M. (2012). Structural features discriminate androgen receptor N/C terminal and coactivator interactions. Mol. Cell. Endocrinol. *348*, 403–410. https://doi.org/10.1016/j.mce.2011.03.026.

Barker, D.J. (1998). In utero programming of chronic disease. Clin. Sci. Lond. Engl. 1979 *95*, 115–128. .

Bedzhov, I., Graham, S.J.L., Leung, C.Y., and Zernicka-Goetz, M. (2014). Developmental plasticity, cell fate specification and morphogenesis in the early mouse embryo. Philos. Trans. R. Soc. Lond. B. Biol. Sci. *369*, 20130538. https://doi.org/10.1098/rstb.2013.0538.

Caldwell, A.S.L., Middleton, L.J., Jimenez, M., Desai, R., McMahon, A.C., Allan, C.M., Handelsman, D.J., and Walters, K.A. (2014). Characterization of Reproductive, Metabolic, and Endocrine Features of Polycystic Ovary Syndrome in Female Hyperandrogenic Mouse Models. Endocrinology *155*, 3146–3159. https://doi.org/10.1210/en.2014-1196.

Cassar, S., Misso, M.L., Hopkins, W.G., Shaw, C.S., Teede, H.J., and Stepto, N.K. (2016). Insulin resistance in polycystic ovary syndrome: a systematic review and meta-analysis of euglycaemic-hyperinsulinaemic clamp studies. Hum. Reprod. Oxf. Engl. *31*, 2619–2631. https://doi.org/10.1093/humrep/dew243.

Chassot, A.-A., Gillot, I., and Chaboissier, M.-C. (2014). R-spondin1, WNT4, and the CTNNB1 signaling pathway: strict control over ovarian differentiation. Reproduction *148*, R97–R110. https://doi.org/10.1530/REP-14-0177.

Cheng, S., Pei, Y., He, L., Peng, G., Reinius, B., Tam, P.P.L., Jing, N., and Deng, Q. (2019). Single-Cell RNA-Seq Reveals Cellular Heterogeneity of Pluripotency Transition and X Chromosome Dynamics during Early Mouse Development. Cell Rep. *26*, 2593-2607.e3. https://doi.org/10.1016/j.celrep.2019.02.031.

Day, F., Karaderi, T., Jones, M.R., Meun, C., He, C., Drong, A., Kraft, P., Lin, N., Huang, H., Broer, L., et al. (2018). Large-scale genome-wide meta-analysis of polycystic ovary syndrome suggests shared genetic architecture for different diagnosis criteria. PLoS Genet. *14*, e1007813. https://doi.org/10.1371/journal.pgen.1007813.

Diamanti-Kandarakis, E., and Dunaif, A. (2012). Insulin resistance and the polycystic ovary syndrome revisited: an update on mechanisms and implications. Endocr. Rev. *33*, 981–1030. https://doi.org/10.1210/er.2011-1034.

Dissen, G.A., Garcia-Rudaz, C., Paredes, A., Mayer, C., Mayerhofer, A., and Ojeda, S.R. (2009). Excessive ovarian production of nerve growth factor facilitates development of cystic ovarian morphology in mice and is a feature of polycystic ovarian syndrome in humans. Endocrinology *150*, 2906–2914. https://doi.org/10.1210/en.2008-1575.

Divoux, A., Erdos, E., Whytock, K., Osborne, T.F., and Smith, S.R. (2022). Transcriptional and DNA Methylation Signatures of Subcutaneous Adipose Tissue and Adipose-Derived Stem Cells in PCOS Women. Cells *11*, 848. https://doi.org/10.3390/cells11050848.

Dumesic, D.A., Oberfield, S.E., Stener-Victorin, E., Marshall, J.C., Laven, J.S., and Legro, R.S. (2015). Scientific Statement on the Diagnostic Criteria, Epidemiology, Pathophysiology, and Molecular Genetics of Polycystic Ovary Syndrome. Endocr. Rev. *36*, 487–525. https://doi.org/10.1210/er.2015-1018.

Dunn, G.A., and Bale, T.L. (2009). Maternal high-fat diet promotes body length increases and insulin insensitivity in second-generation mice. Endocrinology *150*, 4999–5009. https://doi.org/10.1210/en.2009-0500.

Emori, C., and Sugiura, K. (2014). Role of oocyte-derived paracrine factors in follicular development. Anim. Sci. J. *85*, 627–633. https://doi.org/10.1111/asj.12200.

Glintborg, D., Jensen, R.C., Bentsen, K., Schmedes, A.V., Brandslund, I., Kyhl, H.B., Bilenberg, N., and Andersen, M.S. (2018). Testosterone Levels in Third Trimester in Polycystic Ovary Syndrome: Odense Child Cohort. J. Clin. Endocrinol. Metab. *103*, 3819–3827. https://doi.org/10.1210/jc.2018-00889.

Gorry, A., White, D.M., and Franks, S. (2006). Infertility in polycystic ovary syndrome: focus on low-dose gonadotropin treatment. Endocrine *30*, 27–33. https://doi.org/10.1385/ENDO:30:1:27.

Gougeon, A. (1996). Regulation of ovarian follicular development in primates: facts and hypotheses. Endocr. Rev. *17*, 121–155. https://doi.org/10.1210/edrv-17-2-121.

Gu, Y., Runyan, C., Shoemaker, A., Surani, A., and Wylie, C. (2009). Steel factor controls primordial germ cell survival and motility from the time of their specification in the allantois, and provides a continuous niche throughout their migration. Development *136*, 1295–1303. https://doi.org/10.1242/dev.030619.

Hagemann-Jensen, M., Ziegenhain, C., Chen, P., Ramsköld, D., Hendriks, G.-J., Larsson, A.J.M., Faridani, O.R., and Sandberg, R. (2020). Single-cell RNA counting at allele and isoform resolution using Smart-seq3. Nat. Biotechnol. *38*, 708–714. https://doi.org/10.1038/s41587-020-0497-0.

Hammond, G.L. (2016). Plasma steroid-binding proteins: primary gatekeepers of steroid hormone action. J. Endocrinol. *230*, R13–R25. https://doi.org/10.1530/JOE-16-0070.

Houri-Zeevi, L., and Rechavi, O. (2017). A Matter of Time: Small RNAs Regulate the Duration of Epigenetic Inheritance. Trends Genet. TIG *33*, 46–57. https://doi.org/10.1016/j.tig.2016.11.001.

Jin, S., Guerrero-Juarez, C.F., Zhang, L., Chang, I., Ramos, R., Kuan, C.-H., Myung, P., Plikus, M.V., and Nie, Q. (2021). Inference and analysis of cell-cell communication using CellChat. Nat. Commun. *12*, 1088. https://doi.org/10.1038/s41467-021-21246-9.

Kagiwada, S., Kurimoto, K., Hirota, T., Yamaji, M., and Saitou, M. (2013). Replication-coupled passive DNA demethylation for the erasure of genome imprints in mice. EMBO J. *32*, 340–353. https://doi.org/10.1038/emboj.2012.331.

Kelsey, G., Stegle, O., and Reik, W. (2017). Single-cell epigenomics: Recording the past and predicting the future. Science *358*, 69–75. https://doi.org/10.1126/science.aan6826.

Knight, P.G., and Glister, C. (2006). TGF-beta superfamily members and ovarian follicle development. Reprod. Camb. Engl. *132*, 191–206. https://doi.org/10.1530/rep.1.01074.

Kobayashi, H., Sakurai, T., Miura, F., Imai, M., Mochiduki, K., Yanagisawa, E., Sakashita, A., Wakai, T., Suzuki, Y., Ito, T., et al. (2013). High-resolution DNA methylome analysis of primordial germ cells identifies gender-specific reprogramming in mice. Genome Res. *23*, 616–627. https://doi.org/10.1101/gr.148023.112.

Kurimoto, K., Yabuta, Y., Ohinata, Y., Shigeta, M., Yamanaka, K., and Saitou, M. (2008). Complex genome-wide transcription dynamics orchestrated by Blimp1 for the specification of the germ cell lineage in mice. Genes Dev. *22*, 1617–1635. https://doi.org/10.1101/gad.1649908.

Laird, M., Thomson, K., Fenwick, M., Mora, J., Franks, S., and Hardy, K. (2017). Androgen Stimulates Growth of Mouse Preantral Follicles In Vitro: Interaction With Follicle-Stimulating Hormone and With Growth Factors of the TGFβ Superfamily. Endocrinology *158*, 920–935. https://doi.org/10.1210/en.2016-1538.

Lawson, K.A., Dunn, N.R., Roelen, B.A.J., Zeinstra, L.M., Davis, A.M., Wright, C.V.E., Korving, J.P.W.F.M., and Hogan, B.L.M. (1999). Bmp4 is required for the generation of primordial germ cells in the mouse embryo. Genes Dev. *13*, 424–436. .

Lee, H.J., Hore, T.A., and Reik, W. (2014). Reprogramming the methylome: erasing memory and creating diversity. Cell Stem Cell *14*, 710–719. https://doi.org/10.1016/j.stem.2014.05.008.

Li, R., and Albertini, D.F. (2013). The road to maturation: somatic cell interaction and self-organization of the mammalian oocyte. Nat. Rev. Mol. Cell Biol. *14*, 141–152. https://doi.org/10.1038/nrm3531.

Ma, X., Dong, Y., Matzuk, M.M., and Kumar, T.R. (2004). Targeted disruption of luteinizing hormone β-subunit leads to hypogonadism, defects in gonadal steroidogenesis, and infertility. Proc. Natl. Acad. Sci. *101*, 17294–17299. https://doi.org/10.1073/pnas.0404743101.

Maccari, S., Polese, D., Reynaert, M.-L., Amici, T., Morley-Fletcher, S., and Fagioli, F. (2017). Early-life experiences and the development of adult diseases with a focus on mental illness: The Human Birth Theory. Neuroscience *342*, 232–251. https://doi.org/10.1016/j.neuroscience.2016.05.042.

McCartney, C.R., Eagleson, C.A., and Marshall, J.C. (2002). Regulation of gonadotropin secretion: implications for polycystic ovary syndrome. Semin. Reprod. Med. *20*, 317–326. https://doi.org/10.1055/s-2002-36706.

Molyneaux, K.A., Zinszner, H., Kunwar, P.S., Schaible, K., Stebler, J., Sunshine, M.J., O'Brien, W., Raz, E., Littman, D., Wylie, C., et al. (2003). The chemokine SDF1/CXCL12 and its receptor CXCR4 regulate mouse germ cell migration and survival. Development *130*, 4279–4286. https://doi.org/10.1242/dev.00640.

Moore, A.M., Prescott, M., and Campbell, R.E. (2013). Estradiol negative and positive feedback in a prenatal androgen-induced mouse model of polycystic ovarian syndrome. Endocrinology *154*, 796–806. https://doi.org/10.1210/en.2012-1954.

Moore, A.M., Prescott, M., Marshall, C.J., Yip, S.H., and Campbell, R.E. (2015). Enhancement of a robust arcuate GABAergic input to gonadotropin-releasing hormone neurons in a model of polycystic ovarian syndrome. Proc. Natl. Acad. Sci. *112*, 596–601. https://doi.org/10.1073/pnas.1415038112.

Ohinata, Y., Payer, B., O'Carroll, D., Ancelin, K., Ono, Y., Sano, M., Barton, S.C., Obukhanych, T., Nussenzweig, M., Tarakhovsky, A., et al. (2005). Blimp1 is a critical determinant of the germ cell lineage in mice. Nature *436*, 207–213. https://doi.org/10.1038/nature03813.

Ohinata, Y., Ohta, H., Shigeta, M., Yamanaka, K., Wakayama, T., and Saitou, M. (2009). A signaling principle for the specification of the germ cell lineage in mice. Cell *137*, 571–584. https://doi.org/10.1016/j.cell.2009.03.014.

Osorno, R., Tsakiridis, A., Wong, F., Cambray, N., Economou, C., Wilkie, R., Blin, G., Scotting, P.J., Chambers, I., and Wilson, V. (2012). The developmental dismantling of pluripotency is reversed by ectopic Oct4 expression. Dev. Camb. Engl. *139*, 2288–2298. https://doi.org/10.1242/dev.078071.

Petta, S., Ciresi, A., Bianco, J., Geraci, V., Boemi, R., Galvano, L., Magliozzo, F., Merlino, G., Craxì, A., and Giordano, C. (2017). Insulin resistance and hyperandrogenism drive steatosis and fibrosis risk in young females with PCOS. PloS One *12*, e0186136. https://doi.org/10.1371/journal.pone.0186136.

Parekh, S., Ziegenhain, C., Vieth, B., Enard, W., and Hellmann, I. (2018). zUMIs - A fast and flexible pipeline to process RNA sequencing data with UMIs. GigaScience *7*. https://doi.org/10.1093/gigascience/giy059.

Pepling, M.E. (2006). From primordial germ cell to primordial follicle: mammalian female germ cell development. Genes. N. Y. N 2000 *44*, 622–632. https://doi.org/10.1002/dvg.20258.

Picelli, S., Faridani, O.R., Björklund, A.K., Winberg, G., Sagasser, S., and Sandberg, R. (2014). Full-length RNA-seq from single cells using Smart-seq2. Nat. Protoc. *9*, 171–181. https://doi.org/10.1038/nprot.2014.006.

Risal, S., Pei, Y., Lu, H., Manti, M., Fornes, R., Pui, H.-P., Zhao, Z., Massart, J., Ohlsson, C., Lindgren, E., et al. (2019). Prenatal androgen exposure and transgenerational susceptibility to polycystic ovary syndrome. Nat. Med. *25*, 1894–1904. https://doi.org/10.1038/s41591-019-0666-1.

Rivera-Pérez, J.A., and Magnuson, T. (2005). Primitive streak formation in mice is preceded by localized activation of Brachyury and Wnt3. Dev. Biol. *288*, 363–371. https://doi.org/10.1016/j.ydbio.2005.09.012.

Rosenfield, R.L., and Ehrmann, D.A. (2016). The Pathogenesis of Polycystic Ovary Syndrome (PCOS): The Hypothesis of PCOS as Functional Ovarian Hyperandrogenism Revisited. Endocr. Rev. *37*, 467–520. https://doi.org/10.1210/er.2015-1104.

Rossant, J., and Tam, P.P.L. (2004). Emerging Asymmetry and Embryonic Patterning in Early Mouse Development. Dev. Cell *7*, 155–164. https://doi.org/10.1016/j.devcel.2004.07.012.

Rossant, J., and Tam, P.P.L. (2009). Blastocyst lineage formation, early embryonic asymmetries and axis patterning in the mouse. Development *136*, 701–713. https://doi.org/10.1242/dev.017178.

Saitou, M., and Yamaji, M. (2012). Primordial Germ Cells in Mice. Cold Spring Harb. Perspect. Biol. *4*, a008375. https://doi.org/10.1101/cshperspect.a008375.

Seki, Y., Hayashi, K., Itoh, K., Mizugaki, M., Saitou, M., and Matsui, Y. (2005). Extensive and orderly reprogramming of genome-wide chromatin modifications associated with specification and early development of germ cells in mice. Dev. Biol. *278*, 440–458. https://doi.org/10.1016/j.ydbio.2004.11.025.

Sekido, R., and Lovell-Badge, R. (2008). Sex determination involves synergistic action of SRY and SF1 on a specific Sox9 enhancer. Nature *453*, 930–934. https://doi.org/10.1038/nature06944.

Sir-Petermann, T., Maliqueo, M., Angel, B., Lara, H.E., Pérez-Bravo, F., and Recabarren, S.E. (2002). Maternal serum androgens in pregnant women with polycystic ovarian syndrome: possible implications in prenatal androgenization. Hum. Reprod. Oxf. Engl. *17*, 2573–2579. https://doi.org/10.1093/humrep/17.10.2573.

Skinner, M.K., Guerrero-Bosagna, C., Haque, M., Nilsson, E., Bhandari, R., and McCarrey, J.R. (2013). Environmentally induced transgenerational epigenetic reprogramming of primordial germ cells and the subsequent germ line. PloS One *8*, e66318. https://doi.org/10.1371/journal.pone.0066318.

Smith, A. (2017). Formative pluripotency: the executive phase in a developmental continuum. Development *144*, 365–373. https://doi.org/10.1242/dev.142679.

Stener-Victorin, E., Padmanabhan, V., Walters, K.A., Campbell, R.E., Benrick, A., Giacobini, P., Dumesic, D.A., and Abbott, D.H. (2020). Animal Models to Understand the Etiology and Pathophysiology of Polycystic Ovary Syndrome. Endocr. Rev. *41*, bnaa010. https://doi.org/10.1210/endrev/bnaa010.

Streiter, S., Fisch, B., Sabbah, B., Ao, A., and Abir, R. (2016). The importance of neuronal growth factors in the ovary. Mol. Hum. Reprod. *22*, 3–17. https://doi.org/10.1093/molehr/gav057.

Stubbs, S.A., Stark, J., Dilworth, S.M., Franks, S., and Hardy, K. (2007). Abnormal Preantral Folliculogenesis in Polycystic Ovaries Is Associated with Increased Granulosa Cell Division. J. Clin. Endocrinol. Metab. *92*, 4418–4426. https://doi.org/10.1210/jc.2007-0729.

Sugiura, K., Pendola, F.L., and Eppig, J.J. (2005). Oocyte control of metabolic cooperativity between oocytes and companion granulosa cells: energy metabolism. Dev. Biol. *279*, 20–30. https://doi.org/10.1016/j.ydbio.2004.11.027.

Tam, P.P., Loebel, D.A., and Tanaka, S.S. (2006). Building the mouse gastrula: signals, asymmetry and lineages. Curr. Opin. Genet. Dev. *16*, 419–425. https://doi.org/10.1016/j.gde.2006.06.008.

Vincent, J.J., Huang, Y., Chen, P.-Y., Feng, S., Calvopiña, J.H., Nee, K., Lee, S.A., Le, T., Yoon, A.J., Faull, K., et al. (2013). Stage-specific roles for tet1 and tet2 in DNA demethylation in primordial germ cells. Cell Stem Cell *12*, 470–478. https://doi.org/10.1016/j.stem.2013.01.016.

Walters, K.A., Edwards, M.C., Tesic, D., Caldwell, A.S.L., Jimenez, M., Smith, J.T., and Handelsman, D.J. (2018a). The Role of Central Androgen Receptor Actions in Regulating the Hypothalamic-Pituitary-Ovarian Axis. Neuroendocrinology *106*, 389–400. https://doi.org/10.1159/000487762.

Walters, K.A., Gilchrist, R.B., Ledger, W.L., Teede, H.J., Handelsman, D.J., and Campbell, R.E. (2018b). New Perspectives on the Pathogenesis of PCOS: Neuroendocrine Origins. Trends Endocrinol. Metab. *29*, 841–852. https://doi.org/10.1016/j.tem.2018.08.005.

Webber, L., Stubbs, S., Stark, J., Trew, G., Margara, R., Hardy, K., and Franks, S. (2003). Formation and early development of follicles in the polycystic ovary. The Lancet *362*, 1017–1021. https://doi.org/10.1016/S0140-6736(03)14410-8.

Witham, E.A., Meadows, J.D., Shojaei, S., Kauffman, A.S., and Mellon, P.L. (2012). Prenatal Exposure to Low Levels of Androgen Accelerates Female Puberty Onset and Reproductive Senescence in Mice. Endocrinology *153*, 4522–4532. https://doi.org/10.1210/en.2012-1283.

Wu, Y., Yang, S., Ma, J., Chen, Z., Song, G., Rao, D., Cheng, Y., Huang, S., Liu, Y., Jiang, S., et al. (2022). Spatiotemporal Immune Landscape of Colorectal Cancer Liver Metastasis at Single-Cell Level. Cancer Discov. *12*, 134–153. https://doi.org/10.1158/2159-8290.CD-21-0316.

Yamaji, M., Seki, Y., Kurimoto, K., Yabuta, Y., Yuasa, M., Shigeta, M., Yamanaka, K., Ohinata, Y., and Saitou, M. (2008). Critical function of Prdm14 for the establishment of the germ cell lineage in mice. Nat. Genet. *40*, 1016–1022. https://doi.org/10.1038/ng.186.

Yu, H., Pask, A.J., Shaw, G., and Renfree, M.B. (2006). Differential expression of WNT4 in testicular and ovarian development in a marsupial. BMC Dev. Biol. *6*, 44. https://doi.org/10.1186/1471-213X-6-44.

Zhang, B., and Horvath, S. (2005). A general framework for weighted gene co-expression network analysis. Stat. Appl. Genet. Mol. Biol. *4*, Article17. https://doi.org/10.2202/1544-6115.1128.